Novel experimental design for high pressure - high temperature electrical resistance measurements in a 'Paris-Edinburgh' large volume press

Shlomi Matityahu,[1,2,a)] Moran Emuna,[3] Eyal Yahel,[1] Guy Makov,[3] and Yaron Greenberg[1]
[1)] *Department of Physics, NRCN, P.O. Box 9001, Beer-Sheva 84190, Israel*
[2)] *Department of Physics, Ben-Gurion University of the Negev, Beer Sheva 84105, Israel*
[3)] *Department of Materials Engineering, Ben-Gurion University of the Negev, Beer Sheva 84105, Israel*

arXiv:1412.0613v2 [cond-mat.mtrl-sci] 31 Mar 2015

We present a novel experimental design for high sensitivity measurements of the electrical resistance of samples at high pressures (0-6GPa) and high temperatures (300-1000K) in a 'Paris-Edinburgh' type large volume press. Uniquely, the electrical measurements are carried out directly on a small sample, thus greatly increasing the sensitivity of the measurement. The sensitivity to even minor changes in electrical resistance can be used to clearly identify phase transitions in material samples. Electrical resistance measurements are relatively simple and rapid to execute and the efficacy of the present experimental design is demonstrated by measuring the electrical resistance of Pb, Sn and Bi across a wide domain of temperature-pressure phase space and employing it to identify the loci of phase transitions. Based on these results, the phase diagrams of these elements are reconstructed to high accuracy and found to be in excellent agreement with previous studies. In particular, by mapping the locations of several well-studied reference points in the phase diagram of Sn and Bi, it is demonstrated that a standard calibration exists for the temperature and pressure, thus eliminating the need for direct or indirect temperature and pressure measurements. The present technique will allow simple and accurate mapping of phase diagrams under extreme conditions and may be of particular importance in advancing studies of liquid state anomalies.

I. INTRODUCTION

Physical properties of materials under extreme conditions of pressure and temperature have been a subject of increasing interest since the pioneering work of Bridgman in the beginning of the last century.[1] Since then, the pressure-temperature ($P-T$) phase diagrams of a large variety of materials, with particular emphasis on solid-solid and solid-liquid (i.e., the melting curve) phase transitions, have been studied extensively.[2,3] During the last two decades, several studies have observed anomalous behavior of structural, thermal and electrical properties in liquids, driven by pressure and temperature. Prominent examples are the elements phosphorus,[4–6] selenium,[7] sulfur,[8,9] arsenic,[10,11] bismuth,[12,13] tellurium,[14–16] as well as the compounds Yttrium-Alumina $[(Y_2O_3)_x(Al_2O_3)_{1-x}]$[17–20] and water.[21,22] Such anomalies may indicate transitions between different liquid polymorphs, distinguished by short range atomic order.

The study of structural properties in melts, at ambient or at elevated pressure, typically utilizes synchrotron X-ray or neutron radiation.[23–25] However, whereas the identification of structural transitions between solid phases and upon melting is well-developed, the state of the art for determining structure in melts is still evolving.[26,27] Therefore, it is desirable to develop relatively simple and low-cost stand alone table-top measurement techniques to complement the structural studies. There are several alternative techniques suitable for studies of phase transitions in condensed matter at high pressures and temperatures, such as differential thermal analysis (DTA), thermobaric analysis (TBA), ultrasonic measurements, and electrical resistance measurements.[28] Measuring electrical and thermodynamic properties may aid in identifying new transitions or anomalies prior to conducting thorough structural investigations. Furthermore, measurements of electrical and thermodynamic properties form a complementary approach to the investigation of phase transitions which, in conjunction with structural measurements, provide a broad picture of the studied transitions. In the present paper we focus on electrical resistance. This measurement provides an efficient and sensitive probe of structural and electronic transitions, while being relatively simple and straightforward to implement.

Methods for electrical resistance measurements in the $P-T$ phase space were considered in Ref. 29 and two pressure cell configurations suitable for high temperatures electrical resistance measurements using a 'Paris-Edinburgh' (PE) large volume press,[30–35] namely direct and indirect heating configurations, were proposed. The direct heating configuration, meticulously developed in Ref. 29, utilizes a high current directly supplied through the anvils to the sample, and heats it. The sample is wrapped by a cylindrical sleeve (made of graphite in Ref. 29) which does not react with the sample and serves as a pressure-transmitting medium. The electrical resistance of the sample is extracted from the measured voltage drop on the sample-sleeve combined assembly (generated by the high heating current). The indirect heating configuration, on the other hand, utilizes a high heating current supplied through the anvils to a resistive heater.

[a)] Electronic mail: matityas@post.bgu.ac.il

The sample, mounted in a good thermal conducting capsule (usually BN), is insulated from the heater thereby being indirectly heated. The electrical resistance of the sample is measured by means of a separate (small) current, passing to the insulated sample through two metallic electrodes. Due to the small dimensions of the sample, combined with the cell assembly geometry, the indirect heating configuration is more complex to implement in the Paris-Edinburgh large volume press. However, the indirect heating configuration has some substantial advantages, among which are:

(i) Direct measurement of the potential drop across the sample reflects its actual electrical resistance, thereby allowing higher sensitivity to small changes in the electrical resistance of the sample. In the direct heating technique, on the other hand, the measured electrical resistance is the equivalent resistance of the sample-sleeve combined assembly. If the pressure-transmitting medium is made of a conducting material (such as graphite in Ref. 29), the equivalent resistance will be less sensitive to changes in the electrical resistance of the sample alone.

(ii) Indirect heating configuration requires smaller samples resulting in substantially smaller pressure and temperature gradients along the sample.

(iii) In the direct heating configuration, abrupt changes in the electrical resistance of the sample during a phase transition introduce power (hence temperature) instabilities.[36] To overcome this problem, a feedback algorithm involving fast data acquisition electronic system should be introduced.[29] Such a problem does not exist in the indirect heating configuration since the sample is not a part of the heating system. Therefore, the temperature is not affected by any changes in the electrical resistance of the sample.

The applicability of the direct heating configuration to electrical resistance measurements in a PE large volume press has been demonstrated in Ref. 29. We are not aware of similar measurements in the indirect heating configuration. It is thus advantageous to examine the feasibility of this technique and to examine if the potential advantages relative to the direct heating technique can be obtained in practice.

An essential ingredient of high pressure experiments is the determination of the actual pressure and temperature conditions of the sample. Technical issues such as high shear/tensile forces acting on small size samples raise obstacles for a direct measurement of the actual pressure and temperature of the sample. Therefore, a calibration procedure relating the sample pressure and temperature to the external, well-controlled, variables (e.g. external force, oil pressure and heating power) should be employed. It should be emphasized that different cell assemblies and measurement protocols may posses quantitatively different calibrations. Therefore, one should apply a calibration procedure for any new experimental technique or a measurement protocol. The most common calibration method, incorporated in large-scale facilities, utilizes internal calibrants (e.g. NaCl, MgO, Au) for which the equation of state is well known. Two independent calibrants may be used for cross-calibration of pressure and temperature.[37,38] Small-scale laboratories, on the other hand, usually derive a pressure calibration curve by identifying well-defined phase transitions in some elements or compounds (e.g., Bi, Tl, Ba, ZnTe), which serve as pressure reference points.[39] Temperature, in many cases, is directly measured by introducing a radial thermocouple in the vicinity of the sample.[40–43] As opposed to the situation in a multi-anvil high pressure apparatus, the cell assembly in the PE press is uniaxially compressed. As a result, a certain amount of radial flow of the pressurized cell assembly takes place during compression. Such a flow may cause radial displacement of the thermocouple, shifting it away from the sample. A readout of the displaced thermocouple does not reflect the actual temperature of the sample during the experiment. We thus calibrate the temperature in addition to the pressure by using several high temperature reference points in the phase diagrams of Sn and Bi (similarly to Ref. 29).

In the present paper we present a novel experimental setup for electrical resistance measurements of materials at elevated pressures (up to $\approx$ 6GPa) and temperatures (up to $\approx$ 1000K), based on an indirect heating technique using a PE large volume press. The design of such a pressure cell is described. The high sensitivity of the present approach and its utility in identifying phase transitions is demonstrated by measurements on Pb, Sn and Bi. Through consideration of several well-studied reference points in the phase diagrams of Sn and Bi, we determine a calibration curve for the pressure and temperature in our setup, thus eliminating the need for independent measurements of these quantities.

The outline of the paper is as follows: In Sec. II we elaborate on the technical details of the construction of the pressure cell. We describe the experimental setup (Sec. II A) and the sample assembly (Sec. II B). The system performance is examined in Sec. III. Preliminary electrical resistance measurements of Pb, Sn and Bi samples are presented in Sec. III A. The results are discussed and compared to previously published data. We then describe the procedure used to calibrate the actual pressure and temperature of the sample (Sec. III B). The calibration is based on several reference points in the phase diagrams of Sn and Bi. The quality of the measurements and the sample pressure and temperature calibration is tested by constructing the $P-T$ phase diagrams of Pb, Sn and Bi and comparing them with those available in the literature. Finally, we summarize and discuss our results and their implications in Sec. IV.

II. EXPERIMENTAL

A. Experimental setup

In order to control the sample pressure, we utilized the V1-PE large volume press (piston cross section=100cm^2) coupled with a computer controlled hydraulic pump to thrust the pressing piston. The relation between the force F and the oil pressure $P_{\rm oil}$ in our setup is $F = 0.1P_{\rm oil}$, where the oil pressure is measured in bars and the force is measured in ton-force. The oil pressure can be increased up to about 1kbar and is monitored by a pressure transducer. According to Refs. 31 and 44, a pressure gradient of 0.3GPa was found at a pressure of 6GPa, over a distance of 3mm from the center of the cell. Since our sample is only 0.5mm in diameter, it would be reasonable to expect a pressure gradient of $\sim 0.05\%$ over the entire sample.

DC power supply connected to the anvils heats the cylindrical graphite heater (see Fig. 1 and the description in Sec. II B). Power ramping was controlled by a programmable power module connected to the high power supply, by which the heating power increment ΔW, between subsequent data points, is controlled. To dismiss heating rate effects on the amplitude of the discontinuities or the corresponding values of pressure and temperature, every experiment was repeated two to four times with various heating rates of $3.75, 7.5, 11.25, 15$W/min.

The automated control system allows accurate control of pressure and temperature independently. Hence, isobaric or isothermal modes may be performed. A major drawback of the isothermal measurement is that the sample chamber undergoes irreversible deformations during compression and decompression. Such deformations severely limit the number of isothermal runs which may be performed in a given pressure cell assembly. As a result, measurements in a large volume press are usually carried out in an isobaric mode.

At low pressures, percolation of the melt through the BN medium (Fig. 1) is a recurring problem when implementing indirect heating configuration. This problem is more pronounced during the first compression process. In order to avoid sample percolation, we employed a protocol in which the oil pressure is raised to 760bar (which is equivalent to a sample pressure $P \approx 6.3$GPa, see below), followed by a series of isobaric measurements upon decompression. All the results shown below were obtained using this protocol.

B. Sample chamber

A 10mm bi-conical pyrophyllite cell was utilized and the cell assembly is presented in Fig. 1. A cylindrical sample (0.5×0.5mm) was mounted in an electrical insulating h-BN capsule (outer diameter 2.8mm). The BN capsule was mounted within a graphite cylinder (outer diameter 3.5mm) sealed by two graphite disks, which serves as a resistive heater. The graphite heater is electrically connected to the anvils by means of Mo disks and steel rings filled with MgO powder. Heating of the graphite heater is then possible by passing a high current through the anvils. The anvils are maintained at room temperature by external water cooling. Two 0.2mm tungsten electrodes were inserted to contact the sample, via radial drills through the bi-conical pyrophyllite cell. A 0.1mm tungsten wire was coiled around the tungsten electrodes, in order to prevent its disconnection during compression. To avoid contact with the graphite heater the electrical probes were sheathed by Al_2O_3 tubes (⌀0.8mm). AC current, via a well-defined shunt resistor ($R_{shunt} = 500\Omega$), was supplied to the sample and the voltage drop across it was recorded during the entire experiment.

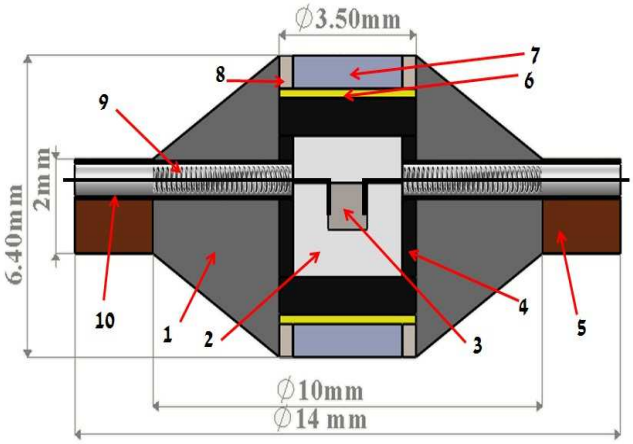

(a)

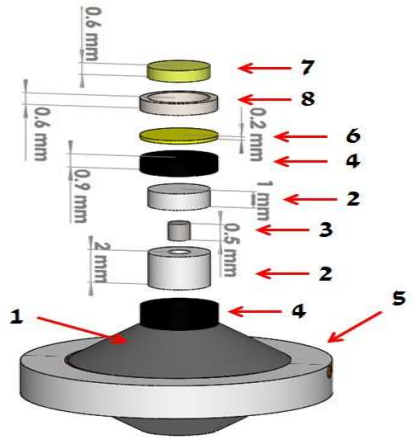

(b)

FIG. 1. (Color online) Schematic of 10mm bi-conical pyrophyllite cell assembly. (a) Cross-cut and (b) "exploded" view. (1) 10mm bi-conical pyrophyllite cell (2) BN sample chamber (3) sample (4) graphite heater (5) Teflon ring (6) Mo disk (7) ceramic insulator (8) steel contact ring (9) coiled tungsten electrode (10) Al_2O_3 sheath tube

III. RESULTS

A. Experimental data

To validate the performance of our experimental design, measurements were carried out on lead (Pb), tin (Sn), and bismuth (Bi) samples. The well-known phase diagrams of these elements exhibit increasing complexity. At moderate pressures, the phase diagram of Pb is characterized by a single solid phase and a melting curve exhibiting a positive slope ($dT_m/dP > 0$), as shown in the inset of Fig. 2.[2,3,45,46] The melting curve of Sn is characterized by a positive slope and includes a solid-solid-liquid triple point (see inset of Fig. 3).[2,3,36,47,48] Finally, the phase diagram of Bi comprises multiple solid phases, transitions in the liquid state,[12,13] and an anomalous melting curve characterized by a negative slope at the low pressures range.[2,3] [see inset of Fig. 4(a)].

Figures 2, 3 and 4 show a series of isobaric measurements of the voltage drop (proportional to the electrical resistance of the sample) across the sample as a function of heating power, measured upon heating of Pb, Sn and Bi samples, respectively. The data obtained upon cooling exhibit the same behavior, apart from an hysteresis characteristic of first-order phase transitions, as shown for the first isobar in Fig. 2.

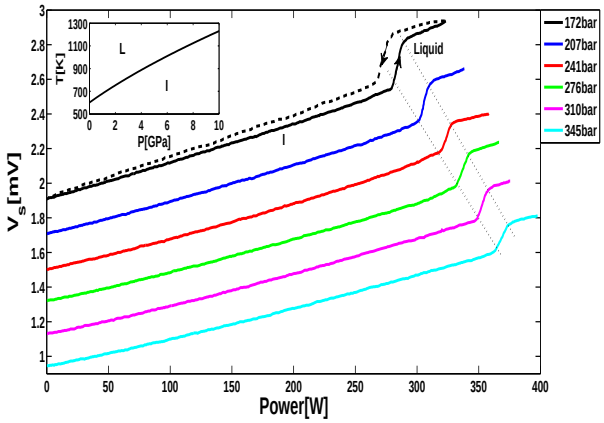

FIG. 2. (Color online) Voltage drop across a Pb sample as a function of heating power at selected oil pressures. For clarity, the curves are vertically biased. The solid (I) and liquid phases are labelled on the first isobar and on the Pb phase diagram in the inset. For the isobar at $P_{\text{oil}} = 172$bar, measurements carried out upon heating (solid curve) and cooling (dashed curve) are presented. Two eye-guiding dotted lines represent the beginning and ending of the melting transition. The small distance between the lines demonstrates the small temperature and pressure gradients across the sample.

The measurements performed on Pb (Fig. 2) exhibit a sharp "step-like" discontinuity which corresponds to a solid-liquid phase transition (melting). The transition temperature increases with pressure, as expected from the positive slope of the melting curve of Pb.[2,3,45,46] At

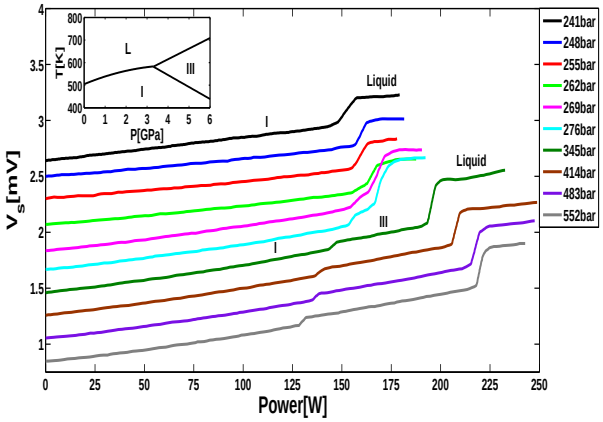

FIG. 3. (Color online) Voltage drop across an Sn sample as a function of heating power at selected oil pressures. For clarity, the curves are vertically biased. The corresponding phases are labelled on selected isobars and the Sn phase diagram in the inset.

low pressures, the Sn measurements (Fig. 3) exhibit a similar trend as Pb. However, an additional phase transition is present at $P_{\text{oil}} \approx 262$bar, accompanied by a smaller discontinuity in the electrical resistance. This point is attributed to the I-III-L triple point in the phase diagram of Sn (see inset of Fig. 3). For $P_{\text{oil}} > 262$bar, the temperature range in which phase III exists enlarges with increasing pressure. Simultaneously, the existence range of phase I decreases.

Results of the electrical resistance measurements of Bi are presented in Fig. 4. The measurements shown in Fig. 4 are in excellent agreement with previous electrical resistance measurements.[49] The transition from a semimetallic phase (phase I) to a metal (phase II) is well-studied[50,51] and is widely used for pressure calibration. This transition is characterized by a sharp drop in electrical resistance.[49,51] Such a sharp drop can be clearly observed in Figs. 4(a) and 4(b). As the pressure increases, this transition occurs at higher heating powers. This implies that the I-II coexistence curve in the $P-T$ phase space is characterized by a negative slope, $dT/dP < 0$. The II-L (melting) transition temperature, on the other hand, exhibits almost no pressure dependence. These findings are in qualitative agreement with the Bi phase diagram [see inset of Fig. 4(a)].

As the pressure increases, the stability range of phase II expands while that of phase I shrinks [see Figs. 4(a) and 4(b)]. At $P_{\text{oil}} \approx 155$bar and above, phase I does not exist above room temperature. The triple point II-VII-L can also be identified from the measurements shown in Fig. 4(b). It is readily seen that at $P_{\text{oil}} \approx 148$bar an additional phase begins to develop before the melting transition, with the transition accompanied by a decrease in the electrical resistance. This discontinuity is associated with the II-VII transition. The range of phase VII increases with increasing pressure, as seen in Fig. 4(c), along with

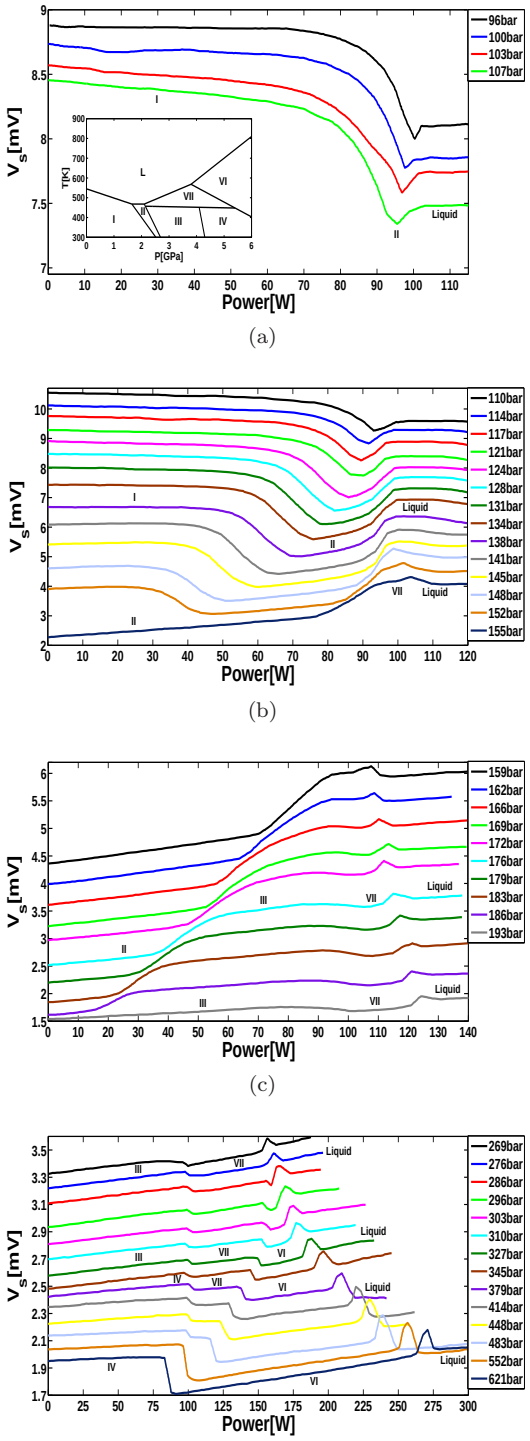

(a)

(b)

(c)

(d)

FIG. 4. (Color online) Voltage drop across a Bi sample as a function of heating power at selected oil pressures. For clarity, the curves are vertically biased. The corresponding phases are labelled on selected isobars and on the Bi phase diagram in the inset of (a).

the appearance of the II-III transition, accompanied by a large increase in the electrical resistance. With increasing pressure, phase II disappears in favor of phase III and the transition temperature strongly decreases with increasing pressure. At $P_{\rm oil} \approx 193$bar phase II does not exist above room temperature. At $P_{\rm oil} \approx 286$bar an additional transition appears before the melting transition, accompanied by a further sharp decrease in the electrical resistance (see Figure 4(d)). This point corresponds to the VI-VII-L triple point. As pressure is further increases, the stability range of phase VI expands while that of phase VII shrinks. The III-VII transition temperature, however, does not shift with increasing pressure. At $P_{\rm oil} \approx 552$bar phase VII is not stable anymore, which indicates the existence of a IV-VI-VII triple point. It should also be noted that the melting curve of phases VII and VI [Figs. 4(c) and 4(d)] is characterized by a positive slope ($dT_m/dP > 0$). All these observations are in line with the Bi phase diagram [inset of Fig. 4(a)].

As mentioned above, measurements were carried out isobarically. Such a thermodynamic path may prevent the detection of the almost vertical coexistence curve of phases III and IV. However, by careful inspection of Fig. 4(d) one may observe a change in the slope dV_s/dW of the low-pressure phase at $P_{\rm oil} \approx 379$bar; the slope dV_s/dW of the low-pressure phase for $P_{\rm oil} \leq 345$bar is slightly larger than that of the low-pressure phase for $P_{\rm oil} \geq 379$bar. This observation suggests that the phase transition III-IV occurs at room temperature for $345\text{bar} < P_{\rm oil} < 379\text{bar}$.

All measurements discussed above incorporate various solid-solid and solid-liquid phase transitions readily identified by clear and sharp discontinuities. These measurements were found to be reproducible upon several heating and cooling cycles. In comparison to measurements in Sn and Bi samples using the direct heating configuration, employed in Ref. 29, the following difference should be emphasized. In the direct heating configuration, phase transitions in Sn and Bi are identified by changes in the slope of the electrical resistance as a function of heating power. In many transitions the change in the slope is rather small, making it difficult to observe phase transitions unambiguously. Two possible sources may contribute to the smearing of the sharp transitions in the direct heating configuration: (i) The electrical resistance of the graphite pressure-transmitting medium which serves as a parasitic resistor connected in parallel to the sample, hence diminishes the sample role in the measured equivalent resistance. (ii) The significant pressure and (especially) temperature gradients across the sample length in the direct heating configuration. These result in a gradient in the electrical resistance of the sample, which smears the sharp discontinuities at phase transitions.

Both of these problems are absent in the indirect heating configuration. The measured electrical resistance is that of the sample itself and the small sample dimensions limit the pressure and temperature gradients. In the next section we use the above measurements to calibrate the sample pressure and temperature in terms of the oil pressure and heating power. Based on this cali-

bration, we then derive the $P-T$ phase diagrams of Pb, Sn and Bi.

B. Pressure and temperature Calibration

As discussed in the introduction, we apply a simple fitting procedure to several reference points in the phase diagrams of Sn and Bi. These reference points are labelled in the insets of Fig. 5(a) and discussed in Sec. III A. To relate the sample pressure and temperature to the oil pressure ($P_{\rm oil}$) and heating power (W), we assume the following relations:[29]

$$P = P_\infty \left(1 - e^{-P_{\rm oil}/P_0}\right), \quad (1)$$

$$T = a(P) \cdot W + T_0. \quad (2)$$

Equation (1) consists of two fitting parameters, P_∞ and P_0, which are assumed to be temperature independent. As in Ref. 29, we found that this assumption remains valid for temperatures up to 1000K, the maximum temperature explored in our experiments. The exponential decay function in Eq. (1) reflects the gasket deformation and accounts for the deviations from linear response at higher pressures.[29] At a given pressure, Eq. (2) assumes a linear variation of the sample temperature as a function of heating power, as verified in previous works.[29,43] The slope of the straight line was shown to be slightly pressure dependent.[29,43] We thus assume $a(P) = a_0 + a_1 P$, where a_0 and a_1 are parameters to be fitted. The parameter T_0 in Eq. (2) describes the sample temperature in the absence of heating power and is taken as $T_0 = 295$K. Variations of ± 10K in this value produce very small changes in the values of the fitting parameters a_0 and a_1.

Following Ref. 29, we first calibrate the sample pressure using six reference points in the phase diagram of Bi and one triple point in the phase diagram of Sn, as labelled in the inset of Fig. 5(a). The fitting parameters are found to be $P_0 = 414$bar and $P_\infty = 7.5$GPa and the corresponding calibration curve is shown in Fig. 5(a). The uncertainty in the sample pressure is estimated to be 5%. Having calibrated the sample pressure, we used a two-dimensional fitting procedure to fit the sample temperature according to Eq. (2). The fitting parameters are found to be $a_0 = 1.82\text{KW}^{-1}$ and $a_1 = -0.027\text{KW}^{-1}\text{GPa}^{-1}$ and the corresponding calibration surface, $T = T(P, W)$, is shown in Fig. 5(b). The uncertainty in the sample temperature is estimated to be 20K.

It should be stressed that the sample pressure and temperature calibration in Fig. 5 applies only for the protocol used in this work, i.e., for a compression to $P_{\rm oil} = 760$bar followed by a decompression process. Indeed, the values of the fitting parameters P_0, P_∞, a_0 and a_1 are quite different from those evaluated in Ref. 29. This may be attributed to inherent differences between the direct and indirect heating configurations, but also to the different protocol used in Ref. 29, in which measurements were performed upon compression.

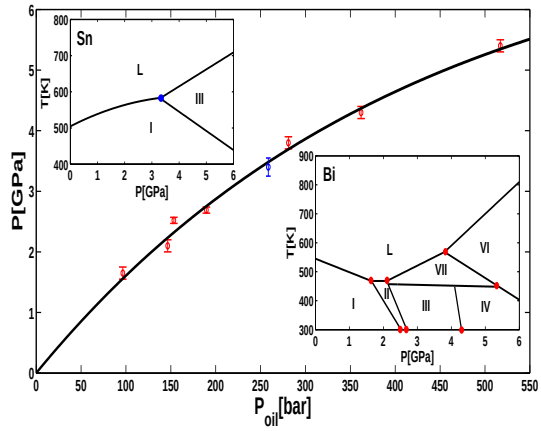

(a)

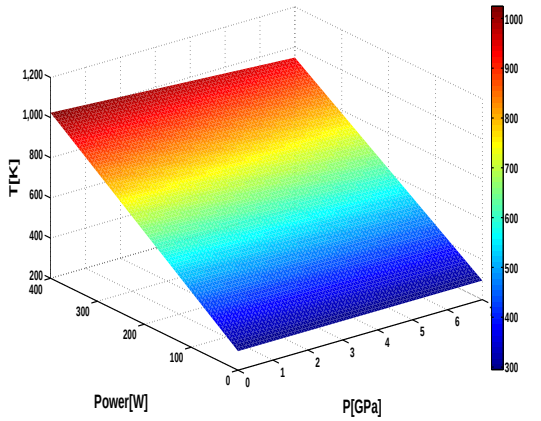

(b)

FIG. 5. (Color online) (a) Sample pressure calibration curve, $P = P(P_{\rm oil})$, derived from a fitting to Eq. (1), based on several reference points in the phase diagrams of Sn and Bi as labelled in the insets. (b) Sample temperature calibration surface, $T = T(P, W)$, derived from a fitting to Eq. (2), based on the high-temperature reference points also used for pressure calibration.

The quality of the calibration procedure and the data in Figs. 2-4 can be examined by constructing the $P-T$ phase diagrams of Pb, Sn and Bi from our electrical resistance measurements. In each of the isobars presented in Figs. 2-4, the values of the oil pressure and heating power corresponding to the onset of the phase transitions were identified. The corresponding sample pressure and temperature were then derived using the calibration presented above. The resulting phase diagrams are shown in Fig. 6. The excellent agreement between the phase diagrams derived from our data and those reported in the literature is clearly evident.[2,3] This demonstrates that the calibration does not vary within our experiments and well-defined relations exist between the sample pressure

and temperature and the oil pressure and heating power within the pressure and temperature range of the experiment (up to 6GPa and 1000K). These relations are well modelled by Eqs. (1) and (2). Additionally, Fig. 6 supports the errors in estimating the sample pressure and temperature indicated above, i.e. ±5% in the sample pressure and ±20K in the sample temperature.

IV. DISCUSSION AND CONCLUSIONS

We have demonstrated a simple, low-cost and sensitive experimental design for measurements of electrical resistance at elevated pressures (up to 6GPa) and temperatures (up to 1000K) using a PE large volume press. The sample is indirectly heated by a resistive graphite heater. A detailed description of the cell assembly is provided. Technical challenges associated with the presented method, namely the disconnection of the metallic electrodes during compression and the percolation of the melt through the BN medium, were considered.

Measurements carried out on Pb, Sn and Bi samples are presented. The measurements are of excellent quality, exhibiting clear discontinuities in the electrical resistance of the sample at phase transitions. These pronounced (nearly abrupt) changes indicate that the pressure and temperature gradients across the sample are very small. These measurements were used to calibrate the sample pressure and temperature as a function of oil pressure and heating power, as well as to validate the performance of the experimental setup. It was found that a calibration independent of sample type exists, thus making independent measurements of the temperature and pressure redundant.

Based on the sample pressure and temperature calibration, the $P-T$ phase diagrams of the above elements were reconstructed and found to be in very good agreement with previously published ones. We have thus shown that accurate electrical resistance measurements can be carried out in a PE large volume press using the indirect heating configuration and may be used to probe phase transitions and anomalous behavior of condensed matter under extreme conditions. Though entailing some technical challenges compared to the direct heating configuration,[29] the quality of the data achieved in the indirect heating configuration is much better. The small dimensions of the sample result in very small pressure and temperature gradients. Furthermore, the indirect heating configuration allows one to probe only the sample, without the effect of the surrounding medium as in the direct heating configuration.[29]

Future experiments with the present method will be aimed at investigations of elemental systems and alloys as well as challenging studies of liquid-liquid phase transitions. In particular, we believe that the high sensitivity of our measurements, even to minor changes in electrical resistance, will allow us to shed more light on liquid-liquid transitions.

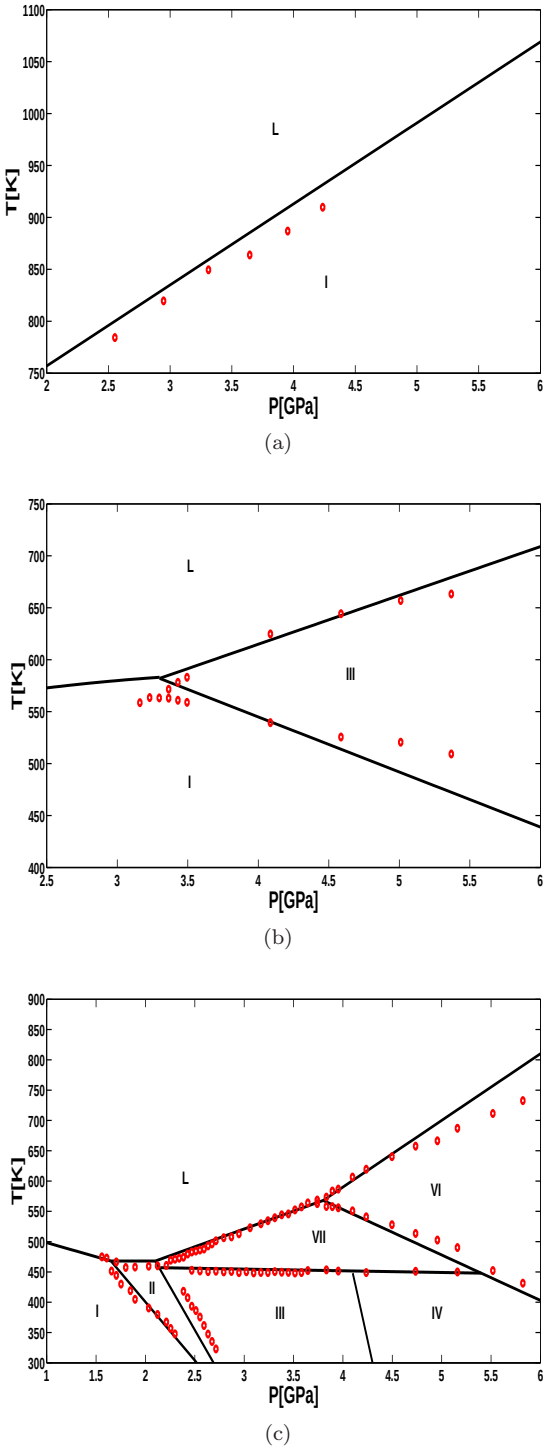

FIG. 6. (Color online) Comparison between the phase diagrams of (a) Pb (b) Sn and (c) Bi derived from our measurements (red points) and those previously published in the literature (solid black lines).[2,3,36,45,49]

ACKNOWLEDGMENTS

We thank S. Klotz, Y. Le Godec, E. Sterer, R. Salem, M. Nikolaevsky, A. Melchior and O. Noked for useful discussions. We also thank A. Damri and E. Sterer for their help in producing cell assembly components.

[1] P. W. Bridgman, *The Physics of High Pressure* (Bell, London, 1931).
[2] D. A. Young, *Phase Diagrams of the Elements* (University of California Press, 1991).
[3] E. Yu. Tonkov and E. G. Ponyatovsky, *Phase Transformations of Elements Under High Pressure* (CRC Press LLC, 2005).
[4] Y. Katayama, T. Mizutani, W. Utsumi, O. Shimomura, M. Yamakata, and K. Funakoshi, Nature (London) **403**, 170 (2000).
[5] G. Monaco, S. Falconi, W. A. Crichton, and M. Mezouar, Phys. Rev. Lett. **90**, 255701 (2003).
[6] S. Falconi, W. A. Crichton, M. Mezouar, G. Monaco, and M. Nardone, Phys. Rev. B **70**, 144109 (2004).
[7] V. V. Brazhkin, S. V. Popova, and R. N. Voloshin, JETP Lett. **50**, 362 (1989).
[8] V. V. Brazhkin, R. N. Voloshin, S. V. Popova, and A. G. Umnov, Phys. Lett. A **154**, 413 (1991).
[9] L. Crapanzano, W. A. Crichton, G. Monaco, R. Bellissent and M. Mezouar, Nat. Mater. **4**, 550 (2005).
[10] Y. Tsuchiya, J. Phys. Condens. Matter **9**, 10087 (1997).
[11] A. Chiba, M. Tomomasa, T. Hayakawa, S. M. Bennington, A. C. Hannon, and K. Tsuji, Phys. Rev. B **80**, R060201 (2009).
[12] A. G. Umnov, V. V. Brazhkin, S. V. Popova, and R. N. Voloshin, J. Phys. Condens. Matter **4**, 1427 (1992).
[13] Y. Greenberg, E. Yahel, E. N. Caspi, C. Benmore, B. Beuneu, M. P. Dariel and G. Makov, Europhys. Lett. **86**, 36004 (2009).
[14] V. V. Brazhkin, R. N. Voloshin, S. V. Popova, and A. G. Umnov, J. Phys. Condens. Matter **4**, 1419 (1992).
[15] K. Yaoita, K. Tsuji, Y. Katayama, N. Koyama, T. Kikegawa, and O. Shimomura, J. Non-Cryst. Solids **156-158**, 157 (1993).
[16] Y. Katayama, K. Tsuji, H. Kanda, H. Nosaka, K. Yaoita, T. Kikegawa, and O. Shimomura, J. Non-Cryst. Solids **205-207**, 451 (1996).
[17] S. Aasland, and P. F. McMillan, Nature (London) **369**, 633 (1994).
[18] G. N. Greaves, M. C. Wilding, S. Fearn, D. Langstaff, F. Kargl, S. Cox, Q. Vu Van, O. Majérus, C. J. Benmore, R. Weber, C. M. Martin, and L. Hennet, Science **322**, 566 (2008).
[19] A. C. Barnes, L. B. Skinner, P. S. Salmon, A. Bytchkov, I. Pozdnyakova, T. O. Farmer, and H. E. Fischer, Phys. Rev. Lett. **103**, 225702 (2009).
[20] G. N. Greaves, M. C. Wilding, D. Langstaff, F. Kargl, L. Hennet, C. J. Benmore, J. K. R. Weber Q. Vu Van, O. Majérus, and P. F. McMillan, J. Non-Cryst. Solids **357**, 435 (2011).
[21] O. Mishima and H. E. Stanely, Nature (London) **396**, 329 (1998).
[22] I. Brovchenko and A. Oleinikova, Chem. Phys. Chem. **9**, 2660 (2008).
[23] Y. Katayama and K. Tsuji, J. Phys. Condens. Matter **15**, 6085 (2003).
[24] A. Filipponi, M. Borowski, D. T. Bowron, S. Ansell, A. Di Cicco, S. De Panfilis, and J-P. Itiè, Rev. Sci. Instrum. **71**, 2422 (2000).
[25] M. Mezouar, P. Faure, W. Crichton, N. Rambert, B. Sitaud, S. Bauchau, and G. Blattmann, Rev. Sci. Instrum. **73**, 3570 (2002).
[26] M. Mayo, E. Yahel, Y. Greenberg, E. N. Caspi, B. Beuneu, G. Makov , J. Appl. Cryst. **46**, 1582 (2013).
[27] P. F. Peterson, E. S. Božin, T. Proffen, and S. J. L. Billinge, J. Appl. Cryst. **36**, 5364 (2003).
[28] M. I. Eremets, *High Pressure Experimental Methods* (Oxford university press, 1996).
[29] E. Principi and A. Di Cicco, Meas. Sci. Technol. **19**, 095701 (2008).
[30] J. M. Besson, R. J. Nelmes, G. Hamel, J. S. Loveday, G. Weill, and S. Hull, Physica B **180181**, 907 (1992).
[31] J. M. Besson and R. J. Nelmes, Physica B **213-214**, 31 (1995).
[32] J. M. Besson, S. Klotz, G. Hamel, I. Makarenko, R. J. Nelmes, J. S. Loveday, R. M. Wilson, and W. G. Marshall, High Press. Res. **14**, 1 (1995).
[33] M. Mezouar, T. Le Bihan, H. Libotte, Y. Le Godec, and D. Häusermann, J. Synchrotron Radiat. **6**, 1115 (1999).
[34] S. Klotz, G. Hamel, and J. Frelat, High Press. Res. **24**, 219 (2004).
[35] A. Yamada, Y. Wang, T. Inoue, W. Yang, C. Park, T. Yu, and G. Shen, Rev. Sci. Instrum. **82**, 015103 (2011).
[36] J. D. Dudley and H. T. Hall, Phys. Rev. **118**, 1211 (1960).
[37] W. Crichton and M. Mezouar, High Temp. - High Press. **34**, 235 (2002).
[38] P. Toulemondea, C. Goujona, L. Laversennea, P. Bordeta, R. Bruyèrea,b, M. Legendrea, O. Leynauda, A. Prata, and M. Mezouar, High Press. Res. **34**, 167 (2013).
[39] D. L. Decker, W. A. Bassett, L. Merrill, H. T. Hall and J. D. Barnett, J. Phys. Chem. Ref. Data **1**, 773 (1972).
[40] S. Wang, D. He, W. Wang, and L. Lei, High Press. Res. **29**, 806 (2009).
[41] Z. Wang, Y. Liu, Y. Bi, W. Song, and H. Xie, High Press. Res. **32**, 167 (2012).
[42] L. Xu, Y. Bi, X. Li, Y. Wang, X. Cao, L. Cai, Z. Wang, and C. Meng, J. Appl. Phys. **115**, 164903 (2014).
[43] Y. Kono, C. Park, C. Kenney-Benson, G. Shen, and Y. Wang, Phys. Earth Planet. Inter. **228**, 269 (2014).
[44] S. Klotz, J. M. Besson, and G. Hamel, High Press. Res. **26**, 277 (2006).
[45] D. Errandonea, J. Appl. Phys. **108**, 033517 (2010).
[46] P. Mirwald and G. Kennedy, J. Phys. Chem. Solids **37**, 795 (1976).
[47] J. D. Barnett, V. E. Bean, and H. T. Hall, J. Appl. Phys. **37**, 875 (1966).
[48] A. I. Kingon and J. B. Clark, High Temp. - High Press. **12**, 75 (1980).
[49] F. P. Bundy, Phys. Rev. **110**, 314 (1958).
[50] P. W. Bridgman, Phys. Rev. **48**, 893 (1935).
[51] P. W. Bridgman, Proc. Am. Acad. Arts Sci. **81**, 167 (1952).